REMOTE SENS. ENVIRON. 32:111–124 (1990)

Spectral Estimates of Net Radiation and Soil Heat Flux

C. S. T. Daughtry

Remote Sensing Research Laboratory, Agricultural Research Service, USDA, Beltsville, Maryland

W. P. Kustas

Hydrology Laboratory, Agricultural Research Service, USDA, Beltsville, Maryland

M. S. Moran, P. J. Pinter, Jr., and R. D. Jackson

U.S. Water Conservation Laboratory, Agricultural Research Service, USDA, Phoenix

P. W. Brown

Department of Soil and Water Science, University of Arizona, Tucson

W. D. Nichols

Water Resources Division, U.S. Geological Survey, Carson City, Nevada

L. W. Gay

School of Renewal Resources, University of Arizona, Tucson

Conventional methods of measuring surface energy balance are point measurements and represent only a small area. Remote sensing offers a potential means of measuring outgoing fluxes over large areas at the spatial resolution of the sensor. The objective of this study was to estimate net radiation (R_n) and soil heat flux (G) using remotely sensed multispectral data acquired from an aircraft over large agricultural fields. Ground-based instruments measured R_n and G at nine locations along the flight lines. Incoming fluxes were also measured by ground-based instruments. Outgoing fluxes were estimated using remotely sensed data. Remote R_n, estimated as the algebraic sum of incoming and outgoing fluxes, slightly underestimated R_n measured by the ground-based net radiometers. The mean absolute errors for remote R_n minus measured R_n were less than 7%. Remote G, estimated as a function of a spectral vegetation index and remote R_n, slightly overestimated measured G; however, the mean absolute error for remote G was 13%. Some of the differences between measured and remote values of R_n and G are associated with

Address correspondence to Dr. C. S. T. Daughtry, USDA-ARS, Remote Sensing Research Lab., Rm. 340, Bldg. 001, BARC-West, Beltsville, MD 20705.

Received 15 September 1989; revised 23 April 1990.

0034-4257/90/$0.00
Published 1990 by Elsevier Science Publishing Co. Inc.

differences in instrument designs and measurement techniques. The root mean square error for available energy ($R_n - G$) was 12%. Thus, methods using both ground-based and remotely sensed data can provide reliable estimates of the available energy which can be partitioned into sensible and latent heat under nonadvective conditions.

INTRODUCTION

Traditional methods of evaluating the energy balance over a large area require an extensive hydrological measurement system. Remote sensing offers a means of measuring outgoing fluxes at a level of detail determined by the spatial resolution of the multispectral sensor (Jackson et al., 1985; Reginato et al., 1985). In the estimation of the surface energy balance under negligible advective conditions with remotely sensed data depends upon the evaluation of the following equation:

$$R_n = LE + H + G, \qquad (1)$$

where LE is latent heat flux, H is sensible heat flux, and G is soil heat flux; all are in W/m^2. The sign convention of Eq. (1) is that LE, H, and G are positive when away from the surface and negative when towards the surface. For R_n the sign convention is opposite to the other three components.

Net radiation (R_n) is the algebraic sum of incoming and outgoing spectral radiant fluxes integrated over all wavelengths, i.e.,

$$R_n = R_{Si} - R_{So} + R_{Li} - R_{Lo}, \qquad (2)$$

where the subscripts S and L signify solar radiation (0.15–4.0 μm) and longwave radiation (> 4.0 μm), respectively. The subscripts i and o indicate, respectively, the incoming and outgoing fluxes relative to the surface. The two incoming fluxes are relatively independent of surface conditions and one set of measurements could represent a large area under stable weather conditions (Jackson et al., 1985). The two outgoing fluxes are highly dependent on surface conditions. For example, both R_{So} and R_{Lo} are considerably different over a well-watered crop from what they are over a dry bare soil for the same incoming fluxes (Kustas et al., 1989).

Previous research has shown that R_n can be calculated from primarily remotely sensed data. Net radiation may be evaluated by combining multispectral estimates of reflected shortwave and emitted longwave radiation with ground-based measurements of incoming shortwave and longwave radiation (Jackson et al., 1985; Kustas et al., 1989). Using different approaches, Jackson (1984) and Brest and Goward (1987) demonstrated how multispectral radiometer data could be used to estimate reflected shortwave radiation or albedo [i.e., R_{So} in Eq. (2)]. Thus, if remotely sensed data are used to evaluate the terms of the radiation balance that depend on surface conditions and ground-based meteorological data are employed to evaluate the remaining terms of Eq. (2), then R_n can be evaluated for large areas.

Soil heat flux is normally measured with heat flow sensors and soil temperature probes buried beneath the soil surface. But, since soil heat flux (G) is highly dependent on surface conditions (i.e., wet or dry and bare or vegetated), it cannot be reliably approximated for large areas. Direct estimation of G by remotely sensed data is not feasible. On a daily basis, soil heat flux is generally small relative to the other fluxes and sometimes has been ignored in energy balance models (e.g., Hatfield et al., 1984). For bare soil, G may be 20–50% of R_n depending on soil moisture (Idso et al., 1975) whereas, for mature crops, G may be 5–10% of R_n under alfalfa (Clothier et al., 1986), wheat (Choudhury et al., 1987), and soybeans (Baldocchi et al., 1985). Thus soil heat flux can be a significant proportion of R_n ranging from 5% to 50% of R_n depending on soil moisture, amount of evidence clearly suggests that the assumption $G = 0$ in Eq. (1) would lead to an overestimate of evaporation and that the magnitude of the overestimate varies with the amount of vegetation (Choudhury et al., 1987). Hence reliable evaluations of the surface energy balance from remote observations require accurate estimates of soil heat flux.

Clothier et al. (1986) estimated the midday ratio of soil heat flux to net radiation (G/R_n) as a linear function of a spectral vegetation index (near IR to red ratio) over several regrowth cycles of alfalfa. Kustas and Daughtry (1990) demonstrated that multispectral data could provide a means of computing the G/R_n ratio for several cover types. In both of the above studies, the G/R_n ratio linearly decreased as vegetative cover and the multispectral vegetation indices increased.

The primary objective of our study was to estimate net radiation and soil heat flux using ground-based meteorological data and remotely sensed multispectral data acquired from an airplane at 150 m over irrigated agricultural fields. The estimates provide a means to evaluate the available energy of the surface ($R_n - G$), which can be partitioned to latent and sensible heat under nonadvective conditions. The remote estimates of G and R_n along flight lines in five fields were compared to point measurements of G and R_n from nine ground-based stations.

EXPERIMENT DESIGN

From 10 to 13 June 1988 an interdisciplinary field experiment was conducted at the University of Arizona Maricopa Agricultural Center (MAC; 33.075°N, 111.983°W) approximately 50 km south of Pheonix, Arizona. Researchers from 19 institutions participated in point measurements of the energy exchange at the soil–plant–atmosphere interface in agricultural fields. Remotely sensed data from ground-based and aircraft-based sensors were employed to obtain a spatial distribution of R_n, LE, H, and G.

Ground-based measurements of air temperature and relative humidity were recorded by an automatic weather station [Campbell Scientific, Inc. (CSI), Logan, Utah[1]] located near the MAC Irrigation Lab. The MAC weather station was centered over a 10 m × 10 m plot of bermudagrass which was surrounded by at least 100 m of dry, fallow ground to the south and east and at least 60 m of packed gravel and sand to the north and west. The temperature and humidity sensor (CSI Model 207) was mounted in a naturally ventilated radiation shield and installed at standard shelter height of 1.5 m. Temperature and humidity measurements were acquired at 1-min intervals from 10 to 15 June 1988.

Soil heat flux and net radiation measurements

Continuous measurements of R_n, G, and soil temperature were recorded at nine locations along transects near the center of five fields (Table 1). The nine flux stations were set up and operated by different teams of investigators and thus the experimental protocol was not standardized from one station to the next. The two cotton fields (28 and 29) and the two bare soil fields (27 and 32) were approximately 300 m wide N–S and 1500 m long E–W while the alfalfa field (21) was 250 m E–W and 750 m N–S. These five fields provided a range of vegetative cover from bare soil to nearly full vegetative canopy cover.

Alfalfa Field 21. The alfalfa (*Medicago sativa* L.) was planted in 1984 and periodically harvested for hay. The vegetative cover was not homogeneous; there are patches of thatch from previous harvests covering the soil. Two weeks prior to our experiment, the alfalfa was cut at 0.1 m and 2 days prior to our experiment the field was flood irrigated, so that the crop was well watered. The

Table 1. Manufacturer (MFG) and Model Number of Net Radiometers and Soil Heat Flux Plates at Each of Nine Stations at MAC[a]

				Net Radiometer			*Soil Heat Flux Plate*			
Field	*Location (m)*	*Station*	*MFG*	*Model*	*Type*	*Height (m)*	*MFG*	*Model*	*No.*	*Depth (cm)*
Cotton 28	670	1	REBS	Q*4	2-dome	1.0	HLW	—	7	5
	680	2	REBS	Q*4	2-dome	1.0	HLW	—	7	5
	900	3	Eppley	PSP + PIR	2-dome	2.0	—	—	—	—
	1100	4	MMI	—	1-dome	1.4	REBS	HFT-3	2	1
Cotton 29	700	8	REBS	Q*4	2-dome	1.0	REBS	HFT-3	5	5
	700	8	MMI	—	1-dome	1.0				
Alfalfa 21	300	6	MMI	—	1-dome	1.0	REBS	HFT-3	2	10
	550	5	MMI	—	1-dome	1.0	REBS	HFT-3	3	5
Soil 27	900	7	MMI	—	1-dome	1.0	REBS	HFT-3	2	10
Soil 32	450	9	MMI	—	1-dome	1.5	REBS	HFT-3	3	5

[a]Abbreviations: Eppley = Eppley Laboratory, Inc., Newport, New Jersey; PSP = precision spectral radiometer (shortwave); PIR = precision infrared radiometer (longwave); MMI = Micromet Instruments, Inc.; REBS = Radiation and Energy Balance Systems, Inc., Renton, Washington; HLW = Made by H. L. Weaver (Weaver and Campbell, 1985).

alfalfa was growing rapidly and plant height increased from 0.43 m to 0.52 m during the experiment (Table 2).

Instruments were located at two sites in field 21. The first site (station 6 in Table 1) was located approximately 300 m from the north end. Two soil heat flux plates were buried 10 cm deep. Changes in heat storage in the soil layer above the heat flux plates were measured by two arrays of four thermocouples wired in parallel to provide spatially averaged soil temperatures. Two of these thermocouple arrays were placed in the soil above the heat flux plates at depths of 2 cm and 7 cm. A net radiometer was placed 1.0 m above a representative area of the canopy. Data were recorded at 10-s intervals and averaged to 12-min means.

The second site (station 5 in Table 1) was located 550 m from the north end of the field. Three soil heat flux plates were buried 5 cm under representative areas of the canopy. One thermocouple was buried midway between each heat flux plate and soil surface. A net radiometer was positioned 1.0 m above the top of the canopy. Data were recorded at 1-min intervals.

Cotton Field 28. Cotton (*Gossypium hirsutum* L., Delta Pine 77) was planted on 29 March 1988. The west half of the field was replanted on 14 April because of poor emergence of the first planting. There were differences in phytomass, leaf area index, and percent cover between the east and west halves of the field (Table 2). Row direction was N–S. Rows were spaced 1.0 m apart with 17 cm deep furrows between each row. The field had been recently irrigated by flooding groups of rows starting at the east end, which resulted in a general increase in surface soil moisture from east to west.

Instruments were located at four sites in field 28. The first and second sites (stations 1 and 2 in Table 1) were located 670 m and 680 m, respectively, from the west end of the field along the dividing line between the older and younger cotton. At each site seven soil heat flux plates were buried 5 cm deep transversing the furrow and parallel to the surface. Thermocouples were inserted midway between the flux plates and the soil surface. One net radiometer was mounted 1.0 m above the canopy near each set of heat flux plates. Data were recorded at 4-s intervals and 6-min means were stored.

The third site (station 3 in Table 1) was located 900 m from the west end of field 28. Two soil heat flux plates, one under the plants in the row and one in the bottom of the furrow, were buried 10 cm deep. Changes in heat storage in the soil layer above the heat flux plates were measured by two thermocouple arrays placed in the soil above the heat flux plates at depths of 2 cm and 7 cm. Incoming and reflected solar radiation were measured with Eppley Precision Spectral Pyranometers, one upright and one inverted. These radiometers have two concentric hemispherical glass domes that transmit radiation in the 285–2800 nm wavelength range. Incoming and emitted longwave (5–50 μm) radiation was measured with Eppley Precision Infrared Radiometers (pyrgeometers), one upright and one inverted. The four radiometers were mounted 2 m above the plant canopy. Data were sampled at 10-s intervals and averaged over 12-min intervals.

The fourth site in field 28 (station 4 in Table 1) was 1100 m from the west end. Two soil heat flux plates were buried 1 cm deep, one in the row under the cotton plants and one in the bottom of

Table 2. Summary of Agronomic Data for Cotton and Alfalfa Fields during the MAC Experiment

Field	*Site*	*Distance (m)*	*Density (Plants / m²)*	*Height (m)*	*Total Dry Phytomass (g / m²)*	*LAI*	*Cover (%)*	*Moisture (%)*
Cotton 28[a]	east	1220	11.8	0.31	58.1	0.42	20	81
Cotton 28[a]	west	655	7.7	0.21	23.9	0.18	11	81
Cotton 29[a]	east	1225	13.6	0.41	120.3	0.83	38	81
Cotton 29[a]	west	645	12.7	0.34	71.5	0.51	21	80
Alfalfa 21[b]	north	290	—	0.44	133.9	—	75	87
Alfalfa 21[b]	south	425	—	0.47	132.5	—	75	86

[a]Cotton data are means of five plants selected from five 3.0-m transects on both 10 and 12 June 1988. Each plant was measured separately ($n = 50$).

[b]Alfalfa data represent means of sixteen 0.25 m² circular samples acquired on both 10 and 13 June 1988 ($n = 32$).

the furrow. One net radiometer was positioned 1.4 m above the canopy. Data were logged at 10-s intervals and averaged to 12-min means.

Cotton Field 29. Cotton (Delta Pine 77) was planted 31 March 1988 with similar furrow orientation and dimensions as field 28. The cotton was larger and more vigorous than the cotton in field 28 (Table 2). The field had been recently cultivated and the soil surface was very dry and cloddy. The field was being irrigated by flooding groups of rows starting at the east end of the field. The portion of the field where station 8 (Table 1) was located was irrigated during the early morning hours of 12 June and had standing water on it until midmorning. Five soil heat flux plates were buried 5 cm deep along a transect between two rows of cotton. Thermocouples were inserted midway between the flux plates and the soil surface. Two net radiometers, a single dome and a double dome, were positioned 1 m above the canopy. Data were recorded at 2-s intervals and 6-min means were stored.

Bare Soil Field 27. The previous wheat crop in field 27 had been harvested and the stubble chisel-plowed twice. The soil surface was rough and cloddy with patches of wheat stubble. Station 7 (Table 1) was located 900 m from the west end of field 27. One net radiometer was mounted 1.0 m above the surface and two soil heat flux plates were buried at 10 cm. Changes in heat storage were measured with thermocouple arrays at 2 cm and 7 cm deep. Data were logged at 10-s intervals and 12-min means were stored.

Bare Soil Field 32. The soil had been smoothed and leveled and appeared uniform and dry. The instruments (station 9 in Table 1) were located 450 m from the west end of the field. Three soil heat flux plates were buried 5 cm deep with a thermocouple located midway between each plate and the soil surface. A single dome net radiometer was positioned 1.5 m above the surface. Data were recorded at 1-min intervals.

Multispectral Reflectance Data

Aircraft-based multispectral data were collected along a flight path that included the five large fields of this study. Two transects along the center of each field were flown from opposite directions so that the mean time of data acquisition for each field coincided within 8 min of the SPOT satellite overpass which occurred at 1133 MST on 11 June and 1114 MST on 12 June 1988. Nominal aircraft altitude was 150 m above ground level.

The airborne sensors included an Exotech 100 (Exotech Inc., Gaithersburg, Maryland[1]) radiometer with SPOT filters, an infrared thermometer (Everest Interscience Inc., Fullerton, California[1]), and a color video camera. The bandpasses of three SPOT filters were 500–590 nm, 610–680 nm, and 790–890 nm and will be referred to as B1, B2, and B3, respectively. The bandpass of the infrared thermometer (IRT) was 8–14 μm and its emissivity was set to 0.98. The multiband radiometer and the IRT both had 15° fields of view (FOV). Information from the video tapes was used to identify the ground location and target composition of each spectral data sample. The instruments were mounted for a view normal to the ground surface. The multispectral data were logged at 1-s intervals during each flight.

The radiance of a painted $BaSO_4$ reference panel was measured by a second Exotech 100 radiometer also with SPOT filters during each flight and was used to calculate reflectance for the aircraft-based data. The voltage output of the ground-based and airborne instruments was compared using the $BaSO_4$ reference panel immediately before and after each flight (Moran et al., 1990).

The normalized difference vegetation index (NDVI) was calculated as the difference in reflectance factors between B3 and B2 divided by their sum. The infrared/red ratio (IRRED) was the ratio of B3 and B2 reflectance factors.

Method for Calculating Soil Heat Flux

Soil heat flux (G) at the surface was estimated by a combination of soil calorimetry and measurement of the heat flux density at the depth given in Table 1 using heat flow plates (Fuchs and Tanner, 1966). Kustas and Daughtry (1990) describe in detail the procedures and corrections used to calculate soil heat flux for this experiment. Briefly, the changes in heat storage of the soil layer above the plate is added to the values measured by the

[1]Company and trade names are given for the benefit of the reader and do not imply any endorsement of the product or company by the U.S. Department of Agriculture.

soil heat flux plate. The volumetric heat capacity, estimated as a function of volume fractions of mineral soil, organic matter, and water (deVries, 1963), was assumed to be constant for the storage layer. Mean temperature of the soil layer above the soil heat flow plates was measured with thermocouples inserted into the soil between the heat flow plates and the soil surface (Table 1). Soil heat flux at the surface above each heat flow plate was evaluated using 0.5 hourly values of soil temperature and measured heat flux at a known depth plus daily estimates of soil moisture. Gravimetric samples for estimating soil moisture in the 0–5 cm layer were collected at midday. Bulk density of the soil in each field was measured on 14 June. Kustas and Daughtry (1990) summarize the soil moisture and bulk density data for each field. The one exception to the above procedure was station 4 in field 28 where the heat flow plates were buried 1 cm deep and the heat storage above the plate was assumed to be negligible. Average soil heat flux at the surface for each station was the mean of the individual measurements of soil heat flux weighted by the area each measurement represented.

Evaluation of Radiation Terms

The net radiation equation [Eq. (2)] can be rewritten in the form

$$R_n = R_{Si} - R_{So} + e_a \sigma T_a^4 - e_s \sigma T_s^4, \qquad (3)$$

where e_a is the effective emissivity for a cloudless sky, σ is the Stefan–Boltzman constant, T_a is the air temperature (°K), e_s is surface emissivity, and T_s is the surface temperature (°K).

Incoming Shortwave Radiation (R_{Si}) or solar radiation was measured with an Eppley Precision Spectral Pyranometer located in field 28. For the nearby cloudless conditions which existed during this experiment a point measurement of R_{Si} should be representative of the entire experimental area.

Outgoing Shortwave Radiation (R_{So}) was estimated by two methods. In the first method, spectral radiances of the scene were measured with an Exotech 100 radiometer with SPOT filters and divided by the partial/total (P/T) ratio to yield total reflected solar radiation (Jackson, 1984). The P/T ratio for the Exotech 100 with SPOT filters is 0.31.

In the second method, albedo was calculated using spectral reflectance factors for representative bands in the visible and near infrared regions (Brest and Goward, 1987). Surfaces were classified as either vegetated or non-vegetated based on the ratio of B3 to B1. For nonvegetated surfaces the B3/B1 ratio was less than 1.5. Because there is no SPOT band in the midinfrared region, an estimate of midinfrared reflectance for vegetation was calculated as 0.5 times the near IR reflectance (i.e., 0.5 B3). For vegetated surfaces Brest and Goward (1987) calculated R_{So} as

$$R_{So} = R_{Si}(0.526\,\mathrm{B1} + 0.418\,\mathrm{B3}). \qquad (4)$$

For nonvegetated surfaces Brest and Goward (1987) calculated R_{So} as

$$R_{So} = R_{Si}(0.526\,\mathrm{B1} + 0.474\,\mathrm{B3}), \qquad (5)$$

where B1 and B3 represent reflectance factors in SPOT bands measured by the Exotech 100 radiometer.

Incoming Longwave Radiation (R_{Li}) was measured with an Eppley Precision Infrared Radiometer (pyrgeometer) located in field 28. Incoming longwave radiation also was calculated using air temperature and humidity data in the following three formulas for R_{Li}: the Idso–Jackson formula (Idso and Jackson, 1969),

$$R_{Li} = \sigma T_a^4 \left\{ 1 - 0.261 \times \exp\left[-7.77 \times 10^{-4} (273 - T_a)^2 \right] \right\}, \qquad (6)$$

the Brutsaert formula (Brutsaert, 1975),

$$R_{Li} = (\sigma T_a^4) 1.24 (e_0 / T_a)^{1/7}, \qquad (7)$$

and the Satterlund formula (Satterlund, 1979),

$$R_{Li} = (\sigma T_a^4) 1.08 [1 - \exp(-e_0 T_a / 2016)], \qquad (8)$$

where σ is the Stefan–Boltzmann constant, T_a is the air temperature at screen height (°K), and e_0 is water vapor pressure (mbars).

Outgoing Longwave Radiation (R_{Lo}). Apparent surface temperatures of the fields were measured with an IRT in the airplane and converted to energy units. The emissivity used by the IRT (i.e., 0.98) to calculate apparent temperature was used to calculate R_{Lo} (Jackson, et al. 1985). This calculation does not require an exact knowledge of surface emissivity.

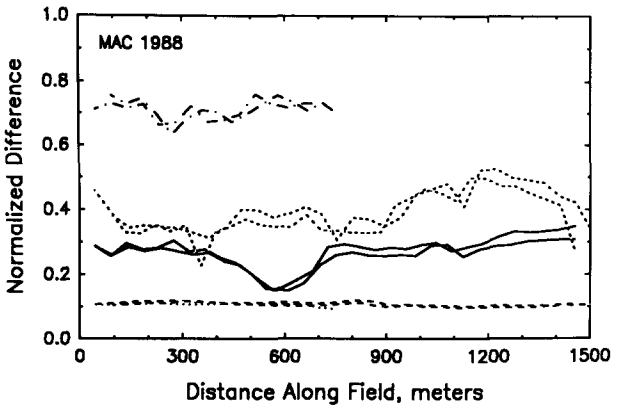

Figure 1. Values of the normalized difference vegetative index (NDVI) along transects through five fields. The multispectral data were acquired from an aircraft at 150 m by a radiometer with SPOT filters. The two transects along the center of each field were flown in opposite directions with mean times of data acquisition that coincided within 8 min of the SPOT satellite overpass on 11 June 1988. (– · –) Alfalfa 21; (—) Cotton 28; (- - -) Cotton 29; (– – –) Soil 32, smooth; (· · ·) Soil 27, rough.

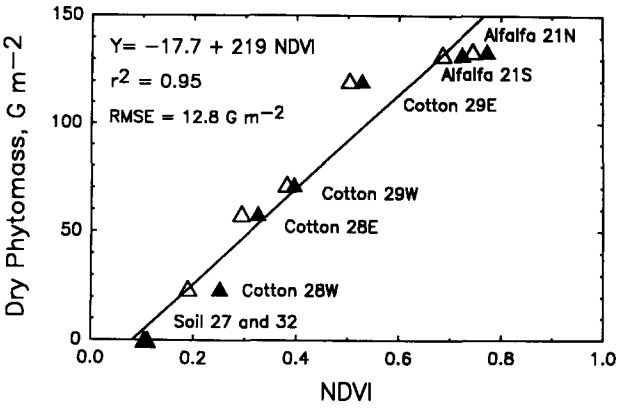

Figure 2. Relationship of total dry phytomass and normalized difference vegetative index (NDVI). The mean time of the aircraft overflight was 1141 and 1111 MST on 11 (△) and 12 (▲) June 1988, respectively.

RESULTS AND DISCUSSION

Agronomic and Surface Reflectance Measurements

Two transects per field were flown in opposite directions immediately before and after the SPOT satellite overpass on 11 and 12 June. Values of the normalized difference vegetation index (NDVI) along the transects through the five fields on 11 June are shown in Figure 1. Alfalfa and the highest NDVI and the bare soil fields had the lowest values.

NDVI of the two cotton fields varied considerably from one end to the other. The dip in NDVI for field 28 between 500 m and 700 m corresponds to a change in plant size which was associated with a change in soil texture from a clay loam to a sandy loam (Huete and Warrick, 1990). The plants growing in the sandy loam soil (28 West in Table 2) were smaller with less total phytomass and leaf area index (LAI) than the plants growing in the clay loam (Cotton 28 East). The lower water holding capacity of the sandy loam soil, compared to the clay loam, probably contributed to the smaller plants.

The NDVI ranking of the fields is consistent with direct measurements of phytomass and LAI in these fields (Table 2). Over the limited range of phytomass in these fields the relationship between phytomass (or LAI) and NDVI is nearly linear (Figure 2). For a wider range of phytomass, the relationship is clearly nonlinear (Hinzman et al., 1986). Mean NDVI for the cotton and alfalfa were slightly, but consistently higher on 12 June than on 11 June. The mean times of the aircraft overflights were 1141 and 1111 MST on 11 and 12 June, respectively, to coincide with SPOT overpass time. Calculations of projected solar angle, which incorporates solar zenith angle and the difference between row azimuth and solar azimuth angles (Kollenkark et al., 1982), indicate that there were approximately 1.7 times more shaded area in the cotton fields on 12 June than on 11 June. Shadows generally increase NDVI by reducing the visible reflectance proportionally more than the near infrared reflectance (Ranson and Daughtry, 1987). The wet soil at the west end (first 300 m) of field 28 also tended to increase the NDVI (Huete and Warrick, 1990). Nevertheless, in this study, NDVI provided a reliable measure of the amount of vegetation present in each field, which is one of the primary factors affecting soil heat flux (Idso et al., 1975; Choudhury et al., 1987).

Net Radiation

Mean conditions at the MAC meteorological station were approximately 1°C warmer and 0.4 kPa drier than in the irrigated cotton field (Table 3). When hourly mean air temperature and vapor pressure data from the MAC meteorological station were used to calculate incoming longwave radiation for 11 and 12 June, the differences between calculated R_{Li} and measured R_{Li} were

Table 3. Mean and Range of Air Temperatures for 11–12 June 1988

Date	Air Temperatures (°C)			Vapor Pressure (kPa)		
	Mean	Min	Max	Mean	Min	Max
			Cotton Field 28			
11 June	27.3	16.0	38.3	0.829	0.636	0.978
12 June	26.5	16.7	34.8	0.926	0.715	1.131
			MAC Weather Station			
11 June	28.4	17.5	39.1	0.473	0.371	0.530
12 June	27.5	17.7	36.2	0.492	0.394	0.543

smaller than when the data from the station in the cotton field were used for two of the three equations (Table 4). Nevertheless, the differences in R_{Li} calculated over the two surfaces were small. The Brutsaert method [Eq. (7)] of calculating R_{Li} on an hourly basis most closely matched measured R_{Li} with the lowest bias and the highest accuracy (lowest $|e|$). The errors were smaller during the night time hours than during the daylight hours, but the ranking of the three models were the same. All three equations for estimating R_{Li} were kept for further analyses.

Spectral estimates of reflected shortwave radiation R_{So} for pixels within 50 m of section 3 in the cotton field were compared to measured values of R_{So} for the four flights. The values of R_{So} calculated by both the Jackson (1984) and the Brest and Goward (1987) models were within 10% of measured R_{So}. Because the sample size was small ($n = 4$), both models for R_{So} were retained for further analyses. Emitted longwave radiation (R_{Lo}) estimated by the airborne infrared thermometer was within 3% of the value measured by an inverted pyrgeometer. Thus the spectral estimates of R_{So} and R_{Lo} were within typical radiation measurement errors without any corrections for the differences in FOV for the remote sensing instruments and the Eppley radiometers.

The "remote R_n" values calculated using the Brest–Goward + Satterlund formulas [Eqs. (3), (4), and (8)] along the transects in each field on 11 June are shown in Figure 3. The triangles represent the "measured R_n" recorded by the ground-based miniature net radiometers described in Table 1. The mean errors for remote R_n minus measured R_n for each station on 11 and 12 June are shown in Table 5. Overall the mean absolute errors between the remote R_n and measured R_n are less than 7% for the Jackson + Brutsaert models and Brest–Goward + Satterlund models (Table 6).

Closer inspection of Tables 5 and 6 reveals several differences among the models in their ability to predict R_n. Net radiation was consistently

Table 4. Means Errors (e), Mean Absolute Errors ($|e|$), and Standard Deviation of Absolute Errors ($SD_{|e|}$) for Hourly Values of Calculated Minus Measured R_{Li} on 11–12 June 1988 ($n = 48$).[a]

Method	Eq.	Cotton Field 28			MAC Weather Station		
		e	$\|e\|$	$SD_{\|e\|}$	e	$\|e\|$	$SD_{\|e\|}$
		W/m^2				W/m^2	
Idso	6	74	74	31	82	82	34
Brutsaert	7	25	25	13	1	8	7
Satterlund	8	53	53	15	42	42	15
		(%)				(%)	
Idso	6	23.1	23.1	9.7	25.6	25.6	10.6
Brutsaert	7	7.8	7.8	4.1	0.3	2.5	2.2
Satterlund	8	16.6	16.3	4.7	13.1	13.1	4.7

[a]Air temperature and vapor pressure were measured in Cotton Field 28 and at the MAC Weather Station. Mean measured long wave radiation was 320 W/m^2.

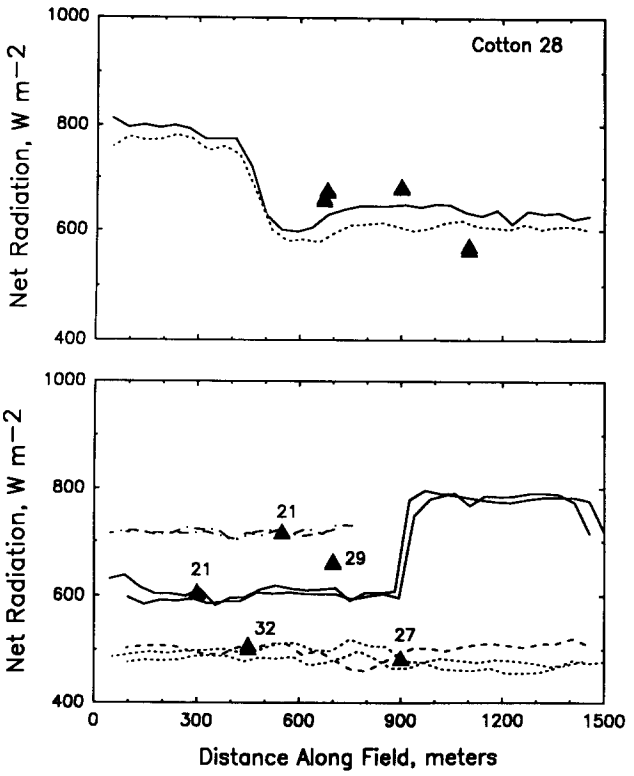

Figure 3. Values of remote net radiation (Brest-Goward + Satterlund formula) along transects through five fields on 11 June 1988. The triangles represent net radiation measured by ground stations in each field. Bottom: (–·–) Alfalfa 21; (—) Cotton 29; (– – –) Soil 27, rough; (- - -) Soil 32, smooth.

overestimated in all fields by models using the Idso–Jackson [Eq. (6)] formula, which overestimated R_{Li} for these conditions. Overall the Jackson + Brutsaert and the Brest–Goward + Satterlund models were comparable and had the lowest mean errors and mean absolute errors (Table 6). The mean R_{Li} predicted by the Brutasert equation during the aircraft overflights was 9 W/m^2 less than R_{Li} measured by the pyrgeometer whereas the Scatterlund equation predicted R_{Li} 35 W/m^2 higher than the pyrgeometer. The mean R_{So} estimated by the Brest–Goward equation was greater than R_{So} estimated by the Jackson method. When the Scatterlund formula for R_{Li} was combined with the Brest Goward formula for R_{So}, the resulting remote R_n (Table 6) was slightly less than the measured R_n and had the greatest accuracy (lowest $|e|$) and highest precision (standard deviation of $|e|$).

Differences between remote R_n and R_n measured by ground-based net radiometers may be expected for a variety of reasons (Jackson et al., 1985). For example, the field of view (FOV) of the multispectral radiometer is 15° whereas the FOV of the miniature net radiometer is approximately 180°. The narrow FOV instrument is likely to see more soil and less vegetation than the wide FOV instrument.

The differences between remote R_n and ground-based R_n measurements should be minimal if all elements of the scene have the same reflectance and are at the same temperature. For the two bare soil fields, mean remote R_n was within 5% of the measured R_n (Table 5). The bare soil fields were relatively homogeneous and differences in FOV of the instruments probably had little effect on values of R_n.

The cotton fields were more complex targets than the bare soil fields. To illustrate the complexity of these targets, surface temperatures of vege-

Table 5. Mean Errors for Remote Net Radiation Minus Measured Net Radiation for Nine Stations at MAC during Overflights on 11–12 June 1988 ($n = 4$)

		Cotton					*Alfalfa*		*Soil*	
		Station								
R_{So} *Eq.*[a]	R_{Li} *Eq.*[b]	*1*	*2*	*3*	*4*	*8*	*6*	*5*	*7*	*9*
						W/m^2				
Jackson	Idso	72	60	74	162	70	248	137	113	95
	Brutsaert	−28	−40	−26	63	−29	148	37	15	−5
	Satterlund	17	5	19	107	15	193	82	59	40
Brest	Idso	15	3	15	103	10	150	29	46	32
	Brutsaert	−84	−97	−85	4	−90	50	−70	−52	−62
	Satterlund	−40	−52	−40	48	−45	95	−26	−8	−23
Measured R_n		651	666	664	573	711	610	728	516	518

[a] Methods of estimating outgoing shortwave radiation: Jackson = Jackson (1984); Brest = Brest and Goward (1987), Eqs. (4) and (5).

[b] Method of estimating incoming longwave radiation: Idso = Idso and Jackson (1969), Eq. (6); Brutsaert = Brutsaert (1975), Eq. (7); Satterlund = Satterlund (1979), Eq. (8).

Table 6. Mean Errors (e), Mean Absolute Errors ($|e|$), and Standard Deviation of Absolute Errors ($SD_{|e|}$) for Remote R_n Minus Measured R_n.[a]

R_{So} Eq.[b]	R_{Li} Eq.[c]	e	$\|e\|$	$SD_{\|e\|}$
			W/m^2	
Jackson	Idso	114	115	62.4
	Brutsaert	15	45	43.6
	Satterlund	59	62	59.5
Brest	Idso	45	48	48.8
	Brutsaert	−54	67	32.0
	Satterlund	−10	44	28.2
			(%)	
Jackson	Idso	18.1	18.3	9.9
	Brutsaert	2.4	7.1	6.9
	Satterlund	9.4	9.8	9.4
Brest	Idso	7.1	7.6	7.7
	Brutsaert	−8.6	10.6	5.1
	Satterlund	−1.6	7.0	4.5

Measured $R_n = 630$ W/m^2

[a] Data are means of nine stations and four overflights on 11–12 June 1988 ($n = 35$, station 7 is missing for one flight on 11 June).
[b] Methods of estimating outgoing shortwave radiation: Jackson = Jackson (1984); Brest = Brest and Goward (1987), Eqs. (4) and (5).
[c] Method of estimating incoming longwave radiation: Idso = Idso and Jackson (1969), Eq. (6); Brutsaert = Brutsaert (1975), Eq. (7); Satterlund = Satterlund (1979), Eq. (8).

tation and sunlit and shaded soil were measured with a hand-held infrared thermometer at nine sites along the flight line in field 28 [Fig. 4A)]. Temperatures of the vegetation were 3–4°C lower than air temperature (T_a). Temperatures of sunlit soil that had recently been irrigated were 3–5°C higher than T_a (i.e., 0–300 m in Fig. 4), while sunlit soil temperatures at the dry end of the field were up to 30°C higher than T_a (i.e., > 500 m in Fig. 4). Shaded soil temperatures ranged from slightly below T_a (wet shaded soil) to nearly 20°C higher than T_a (dry shaded soil). The surface temperature measured by the infrared thermometer in the aircraft was a composite of the temperatures of vegetation and sunlit and shaded soil and was strongly influenced by the pattern of soil moisture measured in the upper 0.05 m [Fig. 4B)]. Huete and Warrick (1990) discuss in detail the soil moisture patterns in field 28.

Mean remote R_n (Brest–Goward + Satterlund formulas) was 6.6% less than the measured R_n for 4 of the five stations in the two cotton fields (Table 5), which is consistent with the conclusions of Jackson et al. (1985) for narrow versus wide FOV instruments. The narrow FOV instruments in the aircraft viewed more warm soil and less vegetation than the wide FOV net radiometers. Thus to a narrow FOV instrument both R_{Lo} and R_{So} should be larger and the remote R_n should be smaller than R_n measured with a net radiometer.

Figure 4. (a) Surface temperatures along two transects through cotton field 28 on 12 June 1988: (—, - - -) temperatures measured by the infrared thermometer in the aircraft; (△) temperatures of sunlit soil (▲) temperature of shaded soil; (▽) temperature of vegetation measured by hand-held infrared thermometers. Air temperature was 33.2°C. (b) Gravimetric soil water content along a transect through field 28 on 12 June 1988.

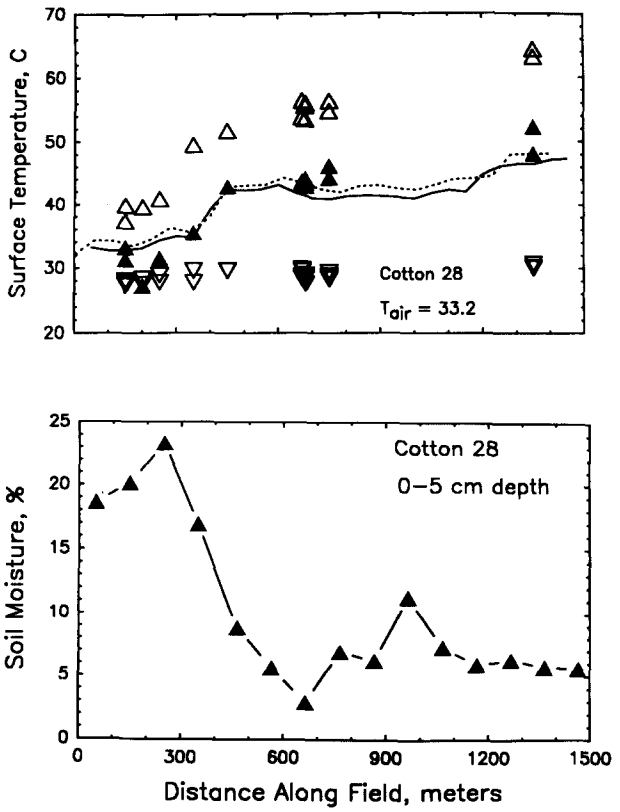

The area surrounding station 8 in cotton field 29 (Table 1) was flood-irrigated during the night of 11 June and the soil surface was saturated during the aircraft overflight on 12 June. The composite surface temperature measured by the airborne infrared thermometer, near station 8 was 51°C (16°C higher than T_a) on 11 June compared to 34°C (less than 1°C higher than T_a) on 12 June. When the incoming and outgoing fluxes are adjusted for the difference in overflight times (0.5 h) for the 2 days, measured R_n increased by 16% (102 W/m^2) after irrigation and remote R_n increased by 21% (129 W/m^2) after irrigation. The lower surface temperatures on 12 June decreased R_{Lo} by 92 W/m^2 and the darker, wet soil decreased R_{So} by 38 W/m^2 (albedo decreased from 0.20 to 0.16) compared with the expected values for a dry surface. Remote R_n (Brest–Goward+ Satterlund) correctly estimated measured R_n at station 8 to within 5%. Thus the abrupt changes in remote R_n in field 29 [(Fig. 3A)] and field 28 [(Fig. 3B)] probably correspond to actual changes in R_n due to irrigation and illustrate how remote sensing can detect spatial variability of R_n.

Another source of differences between remote R_n and measured R_n, which was not addressed in this study, is the errors associated with instrument design, calibration procedures, and measurement techniques. Recent studies have shown that substantial differences exist among various designs of net radiometers (Fritschen and Fritschen, 1989). In this study, both single and double dome miniature net radiometers (Table 1) were employed and operated by the various investigators. Only in cotton field 29 were both types of net radiometers located at the same site. Any effects associated with the net radiometer design and the cover type are confounded and cannot be separated in this study. Nevertheless, the Jackson + Brutsaert model of remote R_n overestimated R_n measured with single dome net radiometers at four or five sites and underestimated R_n measured with double dome net radiometers (Table 5). Although this study cannot provide conclusive evidence, it does suggest that some of the differences in measured R_n may be associated with the design of the net radiometers.

Some of the differences between remote R_n and measured R_n were also related to differences in calibration. Although the most recent calibration constant for each net radiometer was used, there was no attempt to compare all net radiometers over a series of common targets before or after the experiment. The importance of intercalibration of instruments is illustrated by the 112 W/m^2 differences in R_n measured by the two single dome net radiometers in alfalfa field 21 (Fig. 3). However, other evidence strongly suggests that conditions in the alfalfa field were much more homogeneous than indicated by these two net radiometers. First, NDVI for the two sites differed by less than 0.06 units (Fig. 1) which correspond to a 13 g/m^2 (10%) difference in total dry phytomass (Fig. 2). Second, remotely sensed values of R_{So} and R_{Lo} for the two sites differed by only 6 W/m^2 and 8 W/m^2, respectively. Finally, remote R_n for the two sites differed by less than 10 W/m^2 (Table 5). Thus the net radiometer at station 6 in the alfalfa field appears to underestimate R_n by approximately 15% (Fig. 3). In this case, remote R_n was more indicative of the relative differences in R_n in the alfalfa field than the two ground-based net radiometers.

Soil Heat Flux

Remote soil heat flux (remote G) was calculated as a function of remote R_n and the spectral vegetation indices using the following equations proposed by Clothier et al. (1986);

$$G = (0.295 - 0.0133\,\mathrm{IRRED})R_n, \qquad (9)$$

and Kustas and Daughtry (1990),

$$G = (0.294 - 0.0164\,\mathrm{IRRED})R_n \qquad (10)$$

$$G = (0.325 - 0.208\,\mathrm{NDVI})R_n \qquad (11)$$

where IRRED is the ratio of B3 and B2 reflectance factors and NDVI is the difference in reflectance factors between B3 and B2 divided by their sum. Tables 7 and 8 summarize the mean errors for remote G minus measured G for each station. The three remote G models, which used spectral vegetation indices, had similar overall accuracy ($|e|$) (Table 8). The remote G which used NDVI (Kustas and Daughtry, 1990) had the lowest absolute error (13%) with a small positive bias. However, estimating G as simply 10% or 20% of R_n (Tables 7 and 8) generally underestimated measured G. Although the mean G/R_n ratio was 0.24, G/R_n ranged from 0.15 for the recently irrigated cotton to 0.33 for the smooth bare soil. Clearly soil heat flux changes with surface condi-

Table 7. Mean Errors for Remote Soil Heat Flux Minus Soil Heat Flux for Eight Stations at MAC During Overflights on 11–12 June 1988 ($n = 4$)[a]

	Cotton				*Alfalfa*		*Soil*	
	Station							
Model[b]	*1*	*2*	*4*	*8*	*6*	*5*	*7*	*9*
				W/m^2				
Kustas (NDVI)	−3	−16	−11	28	7	−13	52	−7
Kustas (IRRED)	−8	−21	−11	38	22	−9	37	−21
Clothier (IRRED)	−4	−17	−7	43	35	8	39	−19
0.1 R_n	−110	−124	−114	66	−49	−61	−51	−107
0.2 R_n	−49	−62	−52	1	21	10	−1	−57
Measured G	171	185	176	132	120	131	102	156

[a] Net radiation calculated with Brest–Goward plus Satterlund formulas.
[b] Methods of estimating soil heat flux: Kustas = Kustas and Daughtry (1990), $G = (0.325 - 0.208\,\mathrm{NDVI})R_n$ and $G = (0.294 - 0.0164\,\mathrm{IRRED})R_n$. Clothier = Clothier et al. (1986), $G = (0.295 - 0.0133\,\mathrm{IRRED})R_n$

Table 8. Mean Errors (e), Mean Absolute Errors ($|e|$), and Standard Deviations of Absolute Errors ($SD_{|e|}$) for Remote G Minus Measured G Data are Means of Eight Stations and Four Overflights on 11–12 June 1988 ($n = 31$, station 7 is missing for one flight on 11 June)[a]

Model[b]	e	$\|e\|$	$\|e\|$
		W/m^2	
Kustas (NDVI)	−3.2	19.7	17.5
Kustas (IRRED)	−2.2	21.8	17.7
Clothier (IRRED)	8.7	23.2	19.7
0.1R_n	−86.2	86.2	33.6
0.2R_n	−24.3	37.3	23.6
		(%)	
Kustas (NDVI)	2.2	13.3	11.8
Kustas (IRRED)	−1.5	14.7	12.0
Clothier (IRRED)	5.9	15.7	13.3
0.1R_n	−58.2	58.2	22.7
0.2R_n	−16.4	25.2	15.9

[a] Mean measured $G = 148$ W/m^2.
[b] Methods of estimating soil heat flux: Kustas = Kustas and Daughtry (1990); Clothier = Clothier et al. (1986).

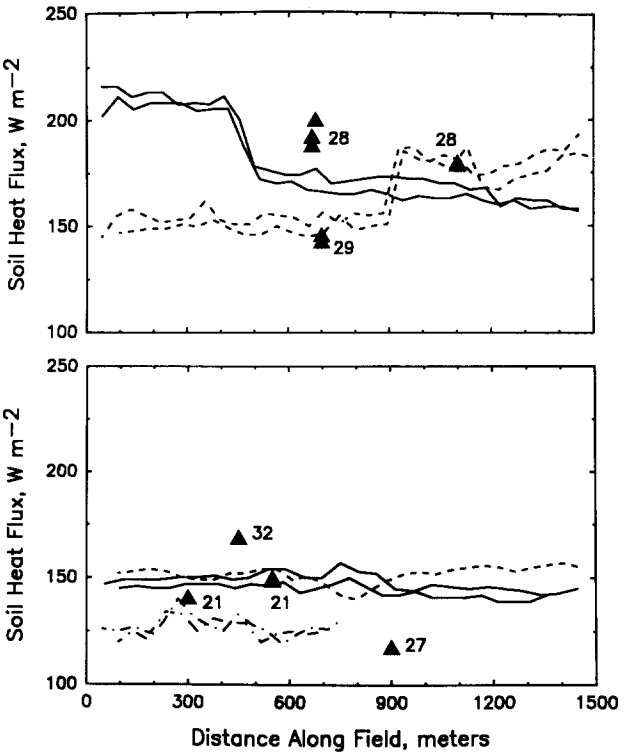

Figure 5. Values of remote soil heat flux ([$G = (0.325 - 0.208\,\mathrm{NDVI})R_n$], Kustas and Daughtry, 1990) along transects through five fields on 11 June 1988: (▲) soil heat flux measured by ground stations in each field. Top: (—) Cotton 28; (– – –) Cotton 29. Bottom (– · –) Alfalfa 21; (– – –) Soil 27, rough; (—) Soil 32, smooth.

tions and estimating G as a constant proportion of R_n without accounting for these effects may result in sizeable errors unless calibrated for each set of conditions.

Transects of remote G and point values of measured G are shown in Figure 5. Remote G consistently underestimated measured G in cotton field 28. The soil heat flux plates at station 4 were buried closer the surface (Table 1) than at the other stations in field 28. When soil heat flux plates are located very near the surface the normal soil heat flux pattern may be distorted which could inflate the measured value of G (Brutsaert, 1982). Problems also may arise from poor contact between the plate and the soil and from possible interference by the plate with water movement in the soil. The furrowed surface of the cotton field also posed the problem of where the plates should be buried and how many plates were needed to characterize the soil heat flux. At station 4, one plate was buried in the row under the cotton

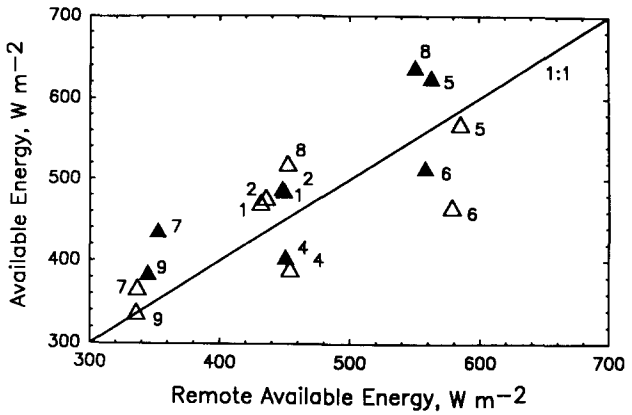

Figure 6. Values of measured available energy ($R_n - G$) versus values of remote available energy (remote R_n − remote G) for nine stations (Table 1) on 11 (△) and 12 (▲) June 1988.

plants and one was buried in the bottom of the furrow. The values of G reported was the mean of the two measurements weighted by the area each represented. At stations 1 and 2, seven plates were buried along a transect between two adjacent rows and the values from each plate were weighted by the area of the transect it represented. The placement and number of plates required to characterize complex surfaces is not well understood.

Available Energy

Available energy is the amount of energy at a surface that can be partitioned into sensible (H) and latent heat (LE) and that can be calculated as $R_n - G$. Values of "remote available energy" (remote R_n − remote G) are plotted as a function of measured available energy for the nine sites in Figure 6. Available energy was lowest in the dry bare soil fields followed by the cotton fields with the dry soil surface. The alfalfa and the recently irrigated cotton (field 29 on 12 June) had the greatest available energy. Irrigation of the cotton field during the night of 11 June increased the available energy of the field by approximately 120 W/m^2 (23%) as more of the incoming radiation was partitioned into latent heat.

The root mean square error (RMSE) for estimating measured available energy from remote available energy was 56 W/m^2 or 12% of the mean (Fig. 6). Thus this technique of using both ground-based and remotely sensed data can provide reliable estimates of the available energy ($R_n - G$) of the surface which can be partitioned into sensible and latent heat under nonadvective conditions.

CONCLUSIONS

Conventional, direct methods of measuring surface energy balance are point measurements and may only represent the surrounding area within which the magnitude of each component is nearly the same. The number of sensors and their placement are crucial to correctly evaluating the components of the energy balance for areas with partial vegetative cover. Remote sensing techniques have the potential advantage of evaluating components of the energy balance over large areas at spatial resolution of the sensor. Incoming fluxes, R_{Si} and R_{Li}, are relatively independent of surface conditions and one set of measurements may represent a large area under stable weather conditions. The outgoing fluxes, R_{So} and R_{Lo}, are highly surface dependent and must be sampled extensively. This study demonstrated that i) reliable areal estimates of R_n and G over very different surfaces can be derived from ground-based and remotely sensed data and ii) this technique can also provide reliable estimates of the available energy ($R_n - G$) of the surface. Thus it appears feasible to estimate the important components of the surface energy balance over large areas with remotely sensed and ground-based data.

This study was a result of the voluntary pooling the resources of several teams of investigators to address issues greater than any single investigator could easily tackle. For future studies we recommend using the same type of net radiometers and soil heat flux plates at all sites within a given experiment or taking steps to minimize confounding the effects of different instrument designs and cover types. Each type of instrument should be calibrated by a common procedure, either in the laboratory or in the field for a series of surfaces spanning the range of anticipated over types. Likewise a uniform protocol for placement and operation of instruments is important to minimize systematic differences.

The MAC experiment was possible only because of the cooperation of the researchers from 19 institutions. Some were in-

volved in the acquisition of the aircraft data, some in the point measurements of the energy exchange, and others in the measurements of plants and soil conditions. Special thanks are due to Mr. Ron Seay and Mr. Tom Clarke, who spent long hours in the heat of the day collecting the plant samples.

REFERENCES

Baldocchi, D. C., Verma, S. B., and Rosenberg, N. J. (1985), Water use efficiency in a soybean field: influence of plant water stress, *Agric. For. Meteorol.* 34:53–65.

Brest, C. L., and Goward, S. N. (1987), Deriving surface albedo measurements from narrow band satellite data, *Int. J. Remote Sens.* 8:351–367.

Brutsaert, W. (1975), On a derivable formula for long-wave radiation from clear skies, *Water Resour. Res.* 11:742–744.

Brutsaert, W. (1982), *Evaporation into the Atmosphere*, Reidel, Boston, 299 pp.

Choudhury, B. J., Idso, S. B., and Reginato, R. J. (1987), Analysis of an empirical model for soil heat flux under a growing wheat crop for estimating evaporation by an infrared-temperature based energy balance equation, *Agric. For. Meteorol.* 39:283–297.

Clothier, B. E., Clawson, K. L., Pinter, P. J., Jr., Moran, M. S., Reginato, R. J., and Jackson, R. D. (1986), Estimation of soil heat flux from net radiation during growth of alfalfa, *Agric. For. Meteorol.* 37:319–329.

deVries, D. A. (1963), Thermal properties of soil, in *Physics of the Plant Environment* (W. R. van Wijk, Ed.), North-Holland, Amsterdam, pp. 210–235.

Fritschen, L. J., and Fritschen, C. L. (1989), Comparison of net radiation measured with various net radiometers, *Agron. Abstr.* 81:14.

Fuchs, M., and Tanner, C. B. (1966), Evaporation from a drying soil, *J. Appl. Meteorol.* 6:852–857.

Hatfield, J.L., Reginato, R. J., and Idso, S. B. (1984), Evaluation of canopy temperature-evapotranspiration models over various crops, *Agric. For. Meteorol.* 32:41–53.

Hinzman, L. D., Bauer, M. E. and Daughtry, C. S. T. (1986), Effects of nitrogen fertilization on growth and reflectance characteristics of winter wheat, *Remote Sens. Environ.* 19:47–61.

Huete, A. R., and Warrick, A. W. (1990), Assessment of vegetation and soil water regimes in partial canopies with optical remotely-sensed data, *Remote Sens. Environ.* (this issue).

Idso, S. B., and Jackson, R. D. (1969), Thermal radiation from the atmosphere *J. Geophys. Res.* 74:5397–5403.

Idos S. B., Aase, J. K. and Jackson, R. D. (1975), Net radiation-soil heat flux relations as influenced by soil water variations, *Boundary-Layer Meteorol.* 9:113–122.

Jackson, R. D. (1984), Total reflected solar radiation calculated from multi-band sensor data, *Agric. For. Meteorol.* 33:163–175.

Jackson, R. D., Pinter, P. J., Jr., and Reginato, R. J. (1985), Net radiation calculated from remote multispectral and ground station meteorological data, *Agric. For. Meteorol.* 35:153–164.

Kollenkark, J. C., Vanderbilt, V. C., Daughtry, C. S. T., and Bauer, M. E (1982), Influence of solar illumination angle on soybean canopy reflectance, *Appl. Opt.* 21:1179–1184.

Kustas, W. P., and Daughtry, C. S. T. (1990), Estimation of the soil heat flux/net radiation ratio from spectral data, *Agric. For. Meteorol.* 49:205–223.

Kustas, W. P., Jackson, R. D., and Asrar, G. (1989), Estimating surface energy-balance components from remotely sensed data, in *Theory and Applications of Optical Remote Sensing* (Ghassem Asrar, Ed.), Wiley, New York, pp. 604–627.

Moran, M. S., Jackson, R. D. Hart, G. F., Slater, P. N., Bartell, B. J., Biggar, S. F., Gellman, D. I., and Santer, R. P. (1990), Obtaining surface reflectance factors from atmospheric and view angle corrected SPOT-1 HRV data, *Remote Sens. Environ.* (this issue).

Ranson, K. J., and Daughtry, C. S. T. (1987), Scene shadow effects on multispectral response, *IEEE Trans. Geosci. Remote Sens.* GE-25:502–509.

Reginato, R. J., Jackson, R. D., and Pinter, P. J., Jr. (1985), Evapotranspiration calculated from remote multispectral and ground station meteorological data, *Remote Sens. Environ.* 18:75–89.

Satterlund, D. R. (1979) An improved equation for estimating long-wave radiation from the atmosphere, *Water Resour. Res.* 15:1649–1650.

Weaver, H. L., and Campbell, G. S. (1985), Use of Peltier coolers as soil heat flux transducers, *Soil Sci. Soc. Am. J.* 49:1065–1067.